Anal Bioanal Chem (2014) 406:7875–7886
DOI 10.1007/s00216-014-8256-z

RESEARCH PAPER

Miniaturized DNA aptamer-based monolithic sorbent for selective extraction of a target analyte coupled on-line to nanoLC

Fabien Brothier · Valérie Pichon

Received: 21 July 2014 / Revised: 1 October 2014 / Accepted: 8 October 2014 / Published online: 22 October 2014

Abstract A complete characterization of a novel target-specific DNA aptamer-based miniaturized solid phase extraction (SPE)-sorbent coupled on-line to nanoLC is presented. A miniaturized oligosorbent (mOS) was prepared via the in situ sol-gel synthesis of a hybrid organic-inorganic monolith in 100 μm i.d. capillary columns using tetraethoxysilane and 3-aminopropyltriethoxysilane as precursors, followed by covalent binding of a 5′-amino-modified DNA aptamer with a C12 spacer arm specific for a molecule of small molecular weight. Ochratoxin A (OTA), one of the most abundant naturally occurring mycotoxins, was chosen as model analyte to demonstrate the principle of such an approach. The mOS was coupled on-line to RP-nanoLC-LIF. Selective extraction of OTA on several mOSs was demonstrated with an average extraction recovery above 80 % when percolating spiked binding buffer and a low recovery on control monoliths grafted with a non-specific aptamer. Reproducibility of mOSs preparation was highlighted by comparing extraction yields. Otherwise, the mOSs demonstrated no cross-reactivity towards an OTA structural analogue, i.e., ochratoxin B. Due to the high specific surface area of the hybrid silica-based monolith, the coverage density of DNA aptamers covalently immobilized in the capillaries was very high and reached 6.27 nmol μL^{-1}, thus leading to a capacity above 5 ng of OTA. This miniaturized device was then applied to the selective extraction of OTA from beer samples. It revealed to be effective in isolating OTA from this complex matrix, thus improving the reliability of its analysis at the trace level.

Keywords Sol-gel monolith · DNA aptamer · Capillary · NanoLC · On-line coupling · Ochratoxin A

Introduction

Solid phase extraction (SPE) is commonly used for sample purification and preconcentration prior to analysis by chromatographic methods. Conventional hydrophobic or polar SPE sorbents may nevertheless be ineffective for removing some interfering compounds from complex matrices. Some matrix constituents may indeed be co-extracted and then co-eluted with the target analyte during the chromatographic separation. To overcome this lack of selectivity, sorbents involving molecular recognition mechanisms have been developed. Among these, extraction sorbents based on the immobilization of biological tools on a solid phase are powerful methods for rapid selection and purification of compounds from complex matrices. The most common approach involving biological tools consists in the use of immunosorbents (IS) based on the specific interaction between an antibody and a target analyte [1–4]. ISs exhibit a high selectivity, high affinity, and a wide range of antigens that can be targeted. Despite these advantages, antibodies are limited by a number of constraints including the use of mammals, long time of regeneration or possible denaturation, and a large molecular size that limits the surface loading and thus the sorbent capacity. More recently, novel-selective sorbents, named oligosorbents (OS), based on the immobilization of aptamers, i.e., short single-stranded oligonucleotides (DNA or RNA), on a solid support have been developed [4–7]. Aptamers are capable of

Electronic supplementary material The online version of this article (doi:10.1007/s00216-014-8256-z) contains supplementary material, which is available to authorized users.

F. Brothier · V. Pichon
Department of Analytical, Bioanalytical Sciences and Miniaturization (LSABM)—UMR CBI 8231 (CNRS-ESPCI), ESPCI ParisTech, PSL Research University, 10 rue Vauquelin, 75231 Paris Cedex 05, France

V. Pichon (✉)
Sorbonne Universités, UPMC, 4 Place Jussieu, 75005 Paris, France
e-mail: valerie.pichon@espci.fr

specifically binding to a target molecule with very high affinities, equivalent to those of antibodies. They are identified in vitro from a large random combinatorial nucleic acid library by an iterative selection process called SELEX [8]. Compared to antibodies, aptamers exhibit many advantages including minimization of the use of animals and regeneration within minutes whereas antibodies recover their active conformation after 1 or 2 days only [1, 4]. They also offer the possibility of introducing some modifications during their chemical synthesis to allow their detection or to facilitate their immobilization on a solid surface [9]. Furthermore, their smaller size (M_w ~3000–20,000) may reduce steric hindrance during the immobilization procedure, thus increasing surface coverage. The choice of the immobilization strategy depends on the nature of the terminal functional group that is available on the aptamers. Three terminal modifications are commercially available: biotin, amine, and thiol [6]. Aptamer immobilization has been mainly achieved using the former one on streptavidin-activated supports for aptamer-based bioassay, affinity chromatography [10–12, 4], or development of OSs for SPE [4, 7, 6, 13]. Due to the simple and strong association between streptavidin and biotin, immobilization is very easy to achieve. However, when using this non-covalent approach, a risk of leakage may occur especially when using organic modifiers that may affect the biotin-streptavidin affinity during the SPE procedure. To overcome these drawbacks, more robust covalent immobilization of amino-modified aptamers was considered. These aptamers consist in oligonucleotides bound via their 5′ or 3′ end to a spacer arm (i.e., tetraethylene glycol or an *n*-alkyl chain C6 or C12) terminated by an amino moiety. In our previous works, 3′ and 5′-C6/C12 amino-modified aptamers specific for cocaine and ochratoxin A (OTA) were successfully grafted on CNBr-activated sepharose microbeads that were then conditioned in disposable SPE cartridges for selective off-line extraction and preconcentration of the target analytes [7, 6, 13, 14]. These OSs offered a higher flexibility concerning the choice of the elution conditions and a good stability for the treatment of biological and food samples.

Nowadays, miniaturization of such SPE sorbents involving DNA or RNA aptamers is of great interest to reduce analytical costs, solvent consumption, and sample volume. Novel strategies are required for immobilizing aptamers in miniaturized devices. Packing of aptamer-grafted microbeads in columns [15–17, 10, 18], chip channels [19, 20], and capillaries [21, 11] has been reported. However, this approach generally involves the use of frits whose synthesis may be tedious for devices of very low diameter [22]. Open tubular capillaries have also been employed to separate proteins or smaller molecules after aptamer immobilization on the inner wall of capillaries [23–30]. The main limitation of this approach resides in the small loading capacity due to the limited surface area of the inner wall [23]. The best compromise consists the use of monolithic supports. These supports present many advantages, among which are fast mass transfer, low back pressure, easier preparation than packed capillaries, and a high surface area available for grafting. Until now, few studies have focused on the grafting of aptamers on miniaturized monolithic devices [31–34]. Grafting has been widely considered using organic monoliths, mainly glycidyl methacrylate-based monoliths, with both biotinylated [32, 33] and amino-modified aptamers [31] for use in affinity chromatography. However, shrinkage and swelling usually affect the stability of such monoliths [35]. Moreover, a complete characterization of the affinity columns in terms of repeatability of the synthesis and of the immobilization procedure is not available. In addition, to our knowledge, no study focused for now on the miniaturization of selective aptamer-based SPE sorbents by using silica-based monoliths. We have recently described the possibility to graft antibodies on a glutaraldehyde-activated hybrid silica-based monolith in situ synthesized in 100 μm i.d. capillaries by sol-gel approach [36]. The obtained miniaturized immunosorbent (mIS) was coupled on-line to nanoLC and characterized. This approach led to reproducible extraction yields and high capacity. The same way of proceeding can be now considered for amino-modified aptamers. N. Deng et al. have recently established short proof of concept of affinity chromatography based on the immobilization of a 5′-C6 amino-modified aptamer specific for a protein, i.e., human α-thrombin, in a 250 μm i.d. capillary after in situ synthesis of this kind of hybrid organic-inorganic monolith [34].

In the present work, a novel-miniaturized aptamer-based SPE sorbent totally coupled on-line to RP-nanoLC (flow rates ≤500 nL min^{-1}) for the analysis of a small molecule from complex samples is presented. The study particularly focused on the complete characterization of the miniaturized oligosorbent (mOS). Particular attention was given to the evaluation of the repeatability of each step which was never carried out in previous works. As previously described by our group for the development of a mIS [36], a hybrid organic-inorganic monolith was in situ synthesized in a 100 μm i.d. capillary. A DNA aptamer specific for a molecule of low molecular weight was covalently bound on this monolith. The monolith was characterized in terms of structure and permeability. Selectivity was checked no only by comparing extraction yields on independent mOSs and controls but also by studying the retention of a structural analogue. The success of the immobilization was confirmed by quantifying aptamers in the grafting solution before and after grafting. Finally, the miniaturized selective tool was applied to the extraction of the target analyte from a complex sample.

OTA was chosen as model analyte. It is an abundant naturally occurring mycotoxin. OTA is nephrotoxic, with carcinogenic properties and possesses teratogenic, immunotoxic, and possible neurotoxic activities [37]. It can easily contaminate food commodities prior to harvest and when improperly stored [38–40]. Cereals (wheat barley,

maize, etc.) and by-products such as beer and breakfast cereals are its major source of intake [41]. It is thus of great interest to develop novel techniques for detection and quantification of OTA in food matrices. The aptamer sequence specific for OTA was identified by Cruz-Aguado and Penner [5]. It demonstrated a very high affinity towards OTA with a dissociation constant in the nanomolar range. The same aptamer sequence was used in sensors [42, 43] and in SPE cartridges [44, 13]. Otherwise, we recently showed that the 5′-C12 amino-modified aptamer enabled to reach higher capacities than a 5′-C6 amino-modified aptamère [13]. The 5′-C12 amino-modified aptamer specific for OTA was thus chosen as model aptamer to make the proof of concept of the miniaturization of OSs in this study.

Materials and methods

Materials and chemicals

Fused silica capillaries (100 μm i.d.×363 μm o.d.) were from Polymicro (Photon Lines, St. Germain en Laye, France). 3-Aminopropyltriethoxysilane (APTES), tetraethyl othosilicate (TEOS), hexadecyltrimethylammonium bromide (CTAB), glutaraldehyde, ochratoxin A (OTA), ochratoxin B (OTB), sodium chloride, K_2HPO_4, Tris–HCl, and $NaCNBH_3$ were from Sigma-Aldrich (Saint-Quentin Fallavier, France). Potassium dihydrogen phosphate (KH_2PO_4) and hydrochloric acid were from VWR (Fontenay-sous-bois, France). Sodium hydroxide (NaOH) was from Merck (Darmstadt, Germany). HPLC-grade acetonitrile, HPLC-grade methanol, and anhydrous ethanol (EtOH) were from Carlo Erba (Val de Reuil, France). High-purity water was obtained using a Milli-Q purification system (Millipore, Saint-Quentin en Yvelines, France). The previously described 5′-amino-modified C12-aptamer specific for OTA (5′-GATCGGGTGTGGGTGGCG TAAAGGGAGCATCGGACA-3′) [13] and cocaine (5′-GGGAGACAAGGAAAATCCTTCAATGAAGTGGGTC GACA-3′) [6] were synthesized and purified by HPLC by Eurogentec (Angers, France).

The binding buffer (BB) consisted of Tris–HCl (10 mM), NaCl (120 mM), KCl (5 mM), and $CaCl_2$ (20 mM). This buffer was always stored and used at 4 °C. The phosphate buffer solution (pH 8.0) consisted of a 0.1 mol L^{-1} of K_2HPO_4 and KH_2PO_4.

Hybrid organic-inorganic monolith synthesis and characterization

Synthesis of the monolith in a capillary

Water and anhydrous ethanol were previously degassed. The procedure was adapted from previous studies [36, 34]. Fused silica capillary was successively rinsed with NaOH 1 mol L^{-1}, HCl 0.2 mol L^{-1}, water, and finally MeOH. The capillary was then purged with nitrogen at 160 °C prior being filled with the polymerization mixture. Polymerization mixture was prepared as follows: 8 mg of CTAB, 32 μL of water, and 215 μL of EtOH are mixed with 112 μL of TEOS and 118 μL of APTES. The polymerization mixture was vortexed prior filling the capillary. Then, with both ends sealed by silicon, the capillary was placed in a 40 °C water bath for 40 h and then rinsed successively with EtOH and water.

Characterization of the monolith

Scanning electron microscopy (SEM) was used to qualitatively characterize the synthesized monolith. The capillary was cut, and its cross-section was observed under a Hitachi S-3600N scanning electron microscope operated with a beam energy comprised between 5 and 20 keV. Permeability measurements were conducted using a nano-pump (NCP-3200RS Nano Pump, Thermo Scientific Dionex) delivering 100 % water ($\eta=10^{-3}$ Pa·s) at different flow rates and allowing to record the resulting backpressure. The permeability was calculated using the Darcy's law which expresses the permeability as a function of the applied flow rate:

$$K = \frac{4 \times \eta \times L}{\pi \times (d_i)^2 \times \Delta P} \times F$$

K is the permeability (m^2), F is the applied flow rate ($m^3\ s^{-1}$), η is the viscosity of the solvent (Pa·s), L the length of the capillary (m), ΔP the measured backpressure (Pa), and finally d_i is the capillary inner diameter (m).

Aptamer immobilization

The procedure was inspired from the methods described for antibody and aptamer immobilization on hybrid organic-inorganic monolith [36, 34]. A solution of glutaraldehyde at 10 % (*v*/*v*) in 100 mM phosphate buffer (pH 8.0) was pumped through a 100-mm-long monolithic capillary column for 16 h at room temperature (RT). The OTA-aptamer solution (1 g L^{-1} in a 200-mM Na_2HPO_4 and 5-mM $MgCl_2$) was heated at 90 °C for 5 min to renaturate the oligonucleotides followed by cooling at room temperature for 30 min. Then, 60 μL of this solution was pumped through the capillary for 25 h at room temperature (RT). The grafted capillary precolumn was then rinsed with 6 μL of phosphate buffer and for 3 h with BB solution containing 5 mg mL^{-1} $NaCNBH_3$. The remaining aldehyde groups were thus deactivated with Tris–HCl contained in the BB solution and the imide reduced to amine by $NaCNBH_3$. The resulting mOS was then rinsed with BB solution and water/ACN (70/30). It was finally filled with BB

and stored at 4 °C for at least 24 h prior being used. The same procedure was applied for the preparation of a mOS specific for cocaine. This latter mOS was used as control. When not in use, the mOSs were always stored at 4 °C in BB solution.

Aptamer quantification

Aptamers in the solutions resulting from the immobilization procedure were quantified by LC-UV. Three solutions were collected, evaporated, and redissolved in known volumes of pure water: solution 1: aptamer solution recovered after grafting and rinsing solution of phosphate buffer; solution 2: rinsing solutions of BB+$NaCNBH_3$ and BB; and solution 3: rinsing solution of water/acetonitrile (70:30).

An Agilent 1200 series (Agilent Technology, Massy, France) LC system equipped with a binary pump, an autosampler, and a diode array detector controlled by Chemstation software was used. Ion pairing chromatography was achieved using a Waters SymmetryShield RP18 column (150 mm×2.1 mm, i.d.; particle size, 3.5 μm, Waters, Saint-Quentin-en-Yvelines, France) maintained at 50 °C with 0.1 M triethylammonium acetate (pH 7) as solvent A and acetonitrile as solvent B. The gradient consisted in a linear increase of the A/B mixture (93:7; *v*/*v*) in 30 min (85.5:14.5; *v*/*v*). The equilibration time of the column was 10 min with the A/B mixture (93:7; *v*/*v*). Aptamers were detected by UV absorbance measurements at 260 nm.

On-line coupling with nanoLC-LIF

Apparatus and nanoLC-LIF analysis

OTA analysis was performed using a system composed of two six-port switching nano-valves (Cheminert nanovolume 6 ports 2 pos 1/32", manual CN2-4346). The first one was connected to the injection loop (250 nL) and to a preconcentration nano-pump (Utimate^{Plus} NanoFlow LC system, LC-Packings, controlled by Chromeleon 6.60 SP9). The second one was connected to the mOS (70×0.1 mm i.d.) placed at the loop position to the analytical nano-pump (NCP-3200RS Nano Pump, Dionex, controlled by Chromeleon 6.80 SR11) and to the analytical column (Chromolith® CapRod® RP-18, 150 mm×0.1 mm i.d., Merck KGaA, Darmstadt, Germany). The mOS was maintained at a temperature of 6 °C with a column oven (TCC 3000RS column compartment, Thermo Scientific Dionex). The analytical column was connected to the LIF detector. Fluorescence excitation radiation was obtained from the 325 nm, 15 mW output of a HeCd laser (Model 3056-M-A02, Melles Griot, Voisins-le-Bretonneux, France) coupled to a Zetalif Evolution LIF detector (Picometrics, Toulouse, France). The nanoLC separation of OTA was achieved in isocratic mode with a mobile phase containing MeCN (30 %) and water (70 %) at a flow rate of 500 nL min^{-1}. All the connections were made thanks to 20 μm i.d. fused silica capillaries (Upchurch Scientific, 360 μm o.d.). Calibration curves were performed by directly connecting the injection loop to the analytical column and the analytical nano-pump using only the first nano-valve.

On-line preconcentration procedure

The sample was loaded in the 250-nL loop. The first nano-valve was switched allowing; thus, the continuous transfer of the sample to the mOS is at a flow rate of 200 nL min^{-1} thanks to the preconcentration nano-pump. This nano-pump delivered the solvent composition necessary for the washing step. After this washing step, the second nano-valve was switched, thus allowing the mobile phase to flow through the mOS (flow rate=500 nL min^{-1}) to disrupt the interactions between the target analyte and the sorbent and finally to transfer the analyte to the analytical column.

Preparation of beer samples

A beer with a 4.2 % ethanol content was chosen. Degassing was performed by sonicating 0.3 L of beer sample for 3 h, previously cooled at 4 °C for 30 min to prevent fast foam formation that may lead to pouring out of sample. The beer was then filtered through a filter paper. A known volume of beer was then diluted once in the same volume of binding buffer (BB) to obtain a beer/BB (50:50) mixture spiked with OTA at different concentration levels: 0.1, 0.3, 0.5, 0.75, 1.0, 1.25, and 1.5 μg mL^{-1}.

Results and discussion

Monolith characterization

The hybrid organic-inorganic monolith was in situ synthesized in 10-cm-long capillary columns (100 μm i.d.) via a one-pot pathway [45–49]. Hydrolysis and co-condensation of two precursors recently used to immobilize antibodies [36], TEOS and APTES, were carried out in the presence of a structure directing agent, i.e., CTAB, that allows the formation of large-through pores. This monolith is thus supposed to exhibit a low backpressure and a homogenous distribution of the amino groups that would not be the case with a postsynthetic functionalization [45, 47–49, 46]. After removal of CTAB, the monolith was characterized in terms of structure and permeability.

Micrographs of the cross-section of the monolith are reported in Fig. 1. As in our previous work [36], it is visible in the first picture that the monolith structure was homogeneous.

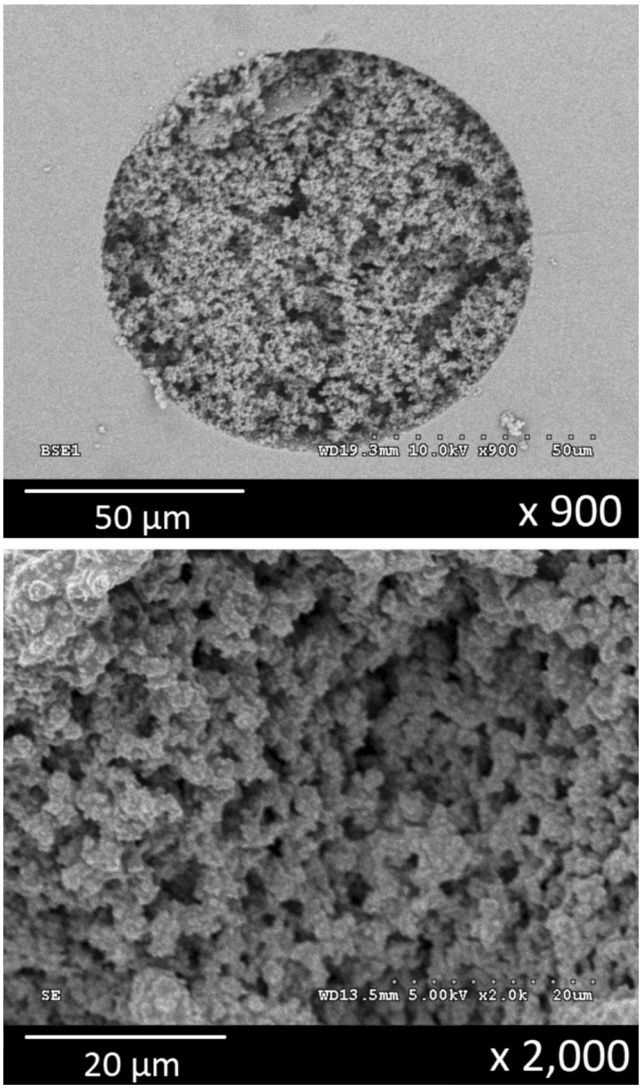

Fig. 1 SEM micrographs (×900, ×2000) of the cross-section of a 100-µm i.d. monolithic support synthesized with APTES and TEOS as precursors

No shrinkage occurred, and the monolith is tightly attached to the capillary inner wall. Otherwise, the monolith is composed of aggregates of silica spheres. Through pores presenting a diameter that comprised between 1 and 2 µm are clearly visible in the picture of magnification 2000. This structure would enable a fast mass transfer and low back pressure.

The backpressure was monitored to get access to the permeability (K) of 12 monolithic capillaries prepared from independent polymerization mixtures by percolating pure water through each monolithic capillary column, thanks to a nano pump. Four different flow rates (F) were applied on each capillary, and the resulting backpressure (ΔP) was recorded. The mean value of permeability was equal to $6.15 \pm 0.67 \times 10^{-14}$ m^2 (RSD=10.9 %, n=12). The generated backpressure of a 7-cm-long capillary column is thus expected to be around 4.8±0.5 bars in pure water or aqueous buffer (such as with an aptamer binding buffer solution) at 200 nL min^{-1} and 12.1± 1.3 bars in an acetonitrile/water (30:70) mobile phase at 500 nL min^{-1}. The structure of the monolith thus allows a low backpressure that is then compatible for on-line coupling. Besides, a RSD value of 10.9 % (n=12) is very satisfying for a silica-based monolith considering the lack of reproducibility of sol-gel synthesis that is generally reported [50].

Optimization of oligoextraction parameters in pure media

Three monolithic capillaries (100 µm i.d.) resulting from three independent sol-gel synthesis were modified by covalently immobilizing OTA aptamers following the procedure illustrated in Fig. 2. The 10-cm-long capillaries were then shortened to a length of 7 cm. The same procedure was applied to cocaine aptamers to constitute three control sorbents. It is thus expected that the controls (i.e., mOSs specific for cocaine) present no affinity for OTA. The resulting anti-OTA mOSs or controls were then placed at the loop position of a six-port switching nano-valve to be connected not only to a preconcentration nano-pump but also to the analytical nano-pump and thus coupled on-line to nanoLC-LIF.

Selectivity of the retention on mOSs

The first step of this study was to optimize the extraction parameters and to compare the retention of OTA on mOSs and controls. To do so, the minimal volume of washing buffer necessary to eliminate possible non-specific interactions was

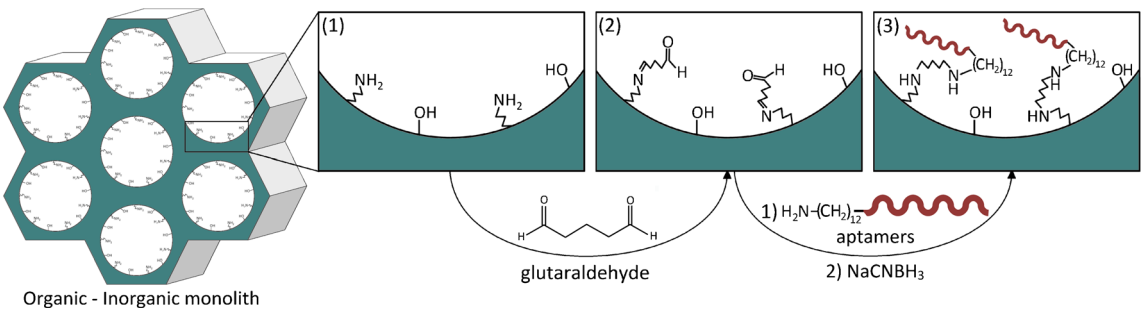

Fig. 2 Immobilization of aptamers on the pores surface of a hybrid organic-inorganic monolith

first determined. This step should allow maintaining a high retention of OTA on the mOSs and its removal from the controls. The washing solution, i.e., BB, allows first the transfer of the full sample volume (250 nL) to the mOS (or control). Washing step begins after percolation of 400 nL BB (250 nL inj.+150 nL void volumes) with the preconcentration nano-pump. Therefore, 250-nL BB spiked at 800 ng mL^{-1} OTA was injected on three mOSs using increasing volume of BB as washing solvent at a flow rate of 200 nL min^{-1} before switching the nano-valve to the inject position to transfer the analyte from the mOS (or control) to the analytical column. The recovery yields of OTA on both sorbents are reported in Table 1.

It is actually visible that the retention remained very high on the three mOSs after washing with 5.0 μL of BB equivalent to more than 11 volumes of the monolithic capillary (assuming a porosity of 0.8 as previously reported [36]). On the contrary, the retention on the three controls quickly decreased. It is thus noticeable that after 1.5–2 μL of washing (i.e., 3.5–4.5 capillary volume), the recovery yields obtained on the controls began to fall. After 5.0 μL of washing with BB, an average recovery of only 14.1±9.5 % on the three controls was obtained against 80.9±7.0 % on the mOSs. This difference demonstrates the selectivity of the retention process of OTA on the mOSs. These results indicate that a washing volume of BB equal to 5.0 μL seems to be at least necessary to remove most of the residual non-specific interactions. Furthermore, the low RSD values (<10.0 %) highlight the high reproducibility of extractions carried out on supports that were independently synthesized. The possibility to graft a DNA aptamer on a hybrid organic-inorganic monolith in a capillary with a reproducible method has thus been demonstrated.

Reproducibility of the extraction procedure

To further investigate the reproducibility of the extraction procedure, it was repeated three times on each mOS and control coupled to nanoLC-LIF with the minimal washing volume required to obtain a high selectivity and previously determined, i.e., 5.0 μL BB. The obtained recovery yields are reported in Fig. 3.

Recovery of 84.8±1.9, 72.8±0.4, and 73.6±9.5 % (n=3) were, respectively, obtained on mOS_1, mOS_2, and mOS_3 when injecting 250 nL of BB spiked at 800 ng mL^{-1} OTA. RSD values were particularly low for mOS_1 and mOS_2 (respectively 2.2 and 0.6 %) and satisfactory for mOS_3 with a RSD of 12.9 %. The repeatability of the extraction protocol was thus highlighted. Furthermore, the recovery yields on $mOS_{1,2,3}$ were not significantly different (ANOVA, p value= 0.07>0.05). It is also noticeable that the recoveries on three controls are low in comparison with mOSs. Extraction yields on $control_{1,2,3}$ of 11.9±3.8, 7.2±5.0, and 25.0±11.6 % (not significantly different, ANOVA: p=0.07>0.05) were obtained. These results again emphasize the high reproducibility of the preparation of the supports and confirm the selectivity of mOSs for OTA.

Evaluation of the cross-reactivity

The aptamer sequence used in this study presents an affinity 100 times higher for OTA than for OTB, the latter being a structural analogue that lacks the chlorine atom in the isocoumarin ring [5]. We have recently described that no specific retention of OTB was observed with the 5′C12 aptamer sequence grafted on sepharose particles that were conditioned in cartridges [13]. Actually, the selectivity resulting from the binding mechanism of the target analyte

Table 1 Comparison of the recovery yields of OTA on three mOSs (70×0.1 mm i.d.) specific for OTA and on three control supports prepared with cocaine aptamers (70×0.1 mm i.d.) after percolation of increasing amounts of BB solution (Tris–HCl (10 mM), NaCl (120 mM), KCl (5 mM), and $CaCl_2$ (20 mM)) during the washing step. Injection of 250 nL of BB spiked at 800 ng mL^{-1} OTA (n=1) onto mOSs and controls coupled on-line with nanoLC/LIF

	$V_{washing}$					
	1.0 μL (%)	1.5 μL (%)	2.0 μL (%)	3.0 μL (%)	4.0 μL (%)	5.0 μL (%)
mOS_1	85.3	93.2	101.9	98.7	89.7	85.7
mOS_2	82.5	91.7	91.0	85.5	74.1	72.9
mOS_3	101.0	108.7	105.4	101.0	78.1	84.1
Average	89.6±10.0	97.8±9.4	99.4±7.5	95.1±8.4	80.7±8.1	80.9±7.0
$Control_1$	94.3	66.4	60.3	43.1	26.9	7.7
$Control_2$	90.3	77.6	57.5	45.7	26.9	9.7
$Control_3$	80.4	85.6	72.6	53.2	40.1	25.0
Average	88.3±7.2	76.5±9.6	63.5±8.0	47.3±5.2	31.3±7.6	14.1±9.5

$V_{washing}$ washing volume

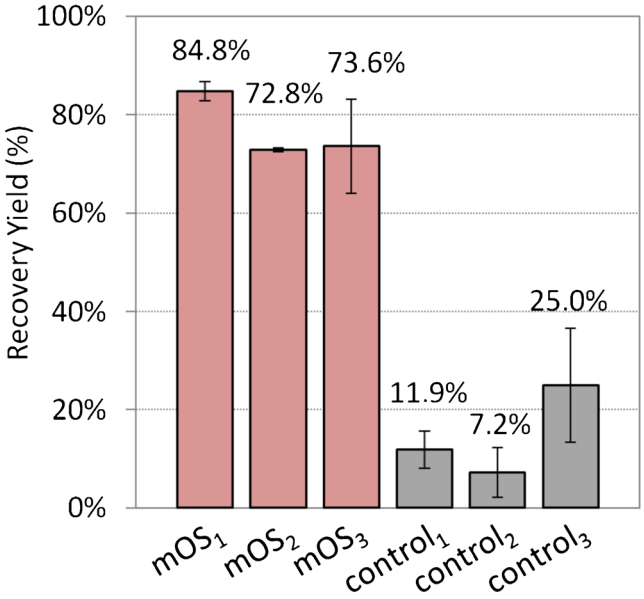

Fig. 3 Reproducibility of the extraction recoveries of OTA on the three mOSs (mOS_1, mOS_2, and mOS_3) specific for OTA and on the three control supports (prepared with cocaine aptamers) coupled on-line with nanoLC-LIF. Injection of 250 nL of BB spiked at 800 ng mL^{-1} OTA. Washing with 5.0 μL BB (n=3)

to its aptamer, i.e., base pair binding in addition with a special conformation of the DNA sequence in the presence of the target analyte, is so high that this aptamer can be used to separate OTA from its analogue. As a consequence, the retention of OTB on a mOS specific for OTA was studied to confirm the selectivity of the miniaturized device towards OTA and further optimize the washing volume of BB finally used. To do so, a fourth mOS, named mOS_4, was synthesized using the same approach as the previous approach used for $mOS_{1,\ 2,\ and\ 3}$. This mOS was then coupled on-line to nanoLC-LIF. BB spiked at 800 ng mL^{-1} OTB was injected on the device (injection loop=250 nL). Figure 4a presents the recovery yields of OTB obtained after various washing volumes with BB. It is visible that the retention of OTB on the mOS quickly fell above 2.0 μL of washing, as previously observed for OTA injections on control capillaries. The recovery after washing with 5.0 μL of BB was equal to 27.8 %, above the average recovery of OTA on controls (14.1±9.5 %, see Table 1). This indicates that the mOS presents a slight selectivity for OTB with a washing volume of 5.0 μL BB. To decrease the retention of OTB on the mOS that is suspected to be only retained by non-specific interactions because of the low affinity of the aptamers for this compound, higher washing volumes of 6.0 and 7.0 μL were considered. Recovery yields of 12.3 and 17.0 % of OTB were obtained respectively. It shows that a washing with at least 6.0 μL of BB seems to be more appropriate to obtain a minimal retention of OTB on the mOS and strongly reduce non-specific interactions. Extraction of OTB and OTA was finally carried out in triplicate after washing with 6.0 μL of BB. The results are presented in Fig. 4b. It is visible that a very high recovery of 88.9±9.6 % was obtained for OTA while a low recovery of only 18.7±6.0 % was observed for OTB on the same mOS. Considering the standard deviation of 9.6 %, the recovery obtained for OTA seems to be similar to the average values previously reported in Table 1 and Fig. 3 with a washing with 5.0 μL of BB. This highlights that retention of OTA remains constant when applying these new conditions of washing. The miniaturized device was thus very specific for OTA and did not exhibit any cross-reactivity towards OTB by using a washing volume of 6.0 μL of BB. This high specificity for OTA confirms that DNA aptamers were successfully grafted on the inorganic-organic monolith and that the total and selective online analysis of a small molecule via the coupling of a miniaturized oligoextraction device with nanoLC is possible.

Determination of the amount of grafted aptamers and binding capacity

The total amount of grafted aptamers was determined by analyzing the amount of non-bonded aptamers in the various solutions applied to the mOS after the grafting procedure. This quantification included the buffer and hydro-organic solutions percolated through the capillary column and that allowed removal of aptamers simply adsorbed at the surface of the monolith. As reported in Table 2, the aptamer density has been determined to be 6.27±0.38 nmol $μL^{-1}$ (R.S.D=6.1 %, n=3) of OTA aptamers in mOSs and 5.14±0.54 nmol $μL^{-1}$ (R.S.D=10.5 %, n=3) of cocaine aptamers in controls. These

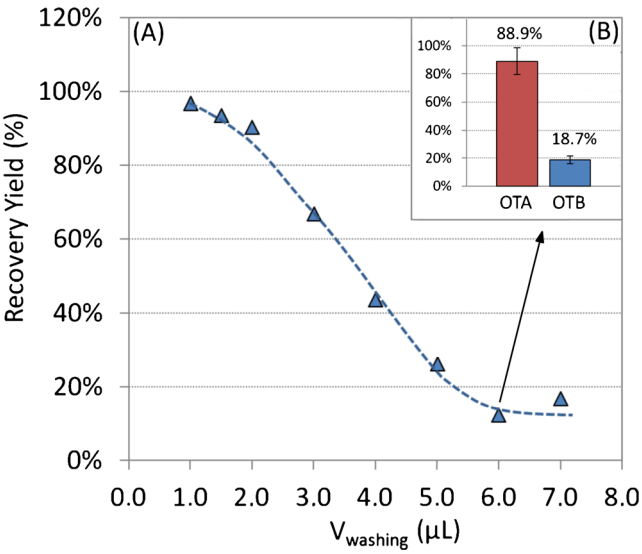

Fig. 4 **A** Recovery yields of OTB on mOS_4 (70×0.1 mm i.d.) specific for OTA coupled on-line with nanoLC/LIF after percolation of increasing amounts of washing solvent: BB solution (Tris–HCl (10 mM), NaCl (120 mM), KCl (5 mM), and $CaCl_2$ (20 mM)). Injection of 250 nL of BB spiked at 800 ng mL^{-1} OTB (n=1). **B** Recovery yields of OTA and OTB on mOS_4 coupled on-line with nanoLC-LIF after washing with 6.0 μL of BB. Injection of 250 nL of BB spiked at 800 ng mL^{-1} OTB or OTA (n=3)

Table 2 Aptamer coverage density and binding capacity of mOSs, controls, and affinity capillary columns developed by Deng and co-workers [34]. Comparison of the grafting conditions and grafting yields

Target analyte	mOS OTA	Control Cocaine	Deng et al. [34] Thrombin
Grafted aptamers			
Spacer arm	C12	C12	C6
Coverage density (nmol μL^{-1})	6.27±0.38	5.14±0.54	0.568
RSD (n=3) (%)	6.10	10.50	13.50
Binding capacity (pmol μL^{-1})	≥22.5	n.d	30.7
Grafting conditions			
Capillary i.d. (μm)	100	100	250
Capillary length (cm)	10	10	10
Activation (h)	16	16	n.c.
$T°_{grafting}$	RT°	RT°	4 °C
Grafting time (h)	25	25	24
$C°_{aptamer}$ (μM)	86.4	82.7	25
$Qty_{apt.\ perc.}$ (nmol)	5.2	5.0	5.7
$Qty_{apt.\ perc.}/V_{cap}$ (nmol μL^{-1})	6.6	6.3	1.2[a]
Grafting yield (%)	96.4±1.6	83.3±9.1	48.9[a]

$C°_{aptamer}$ concentration of aptamers in the grafting solution, V_{cap} volume of the empty capillary, $Qty_{apt.\ perc.}$ total amount of percolated aptamers, $Qty_{apt.\ perc.}/V_{cap}$. theoretical maximal achievable coverage density, *RT* room temperature

[a] Deduced from the reported data

results are 9 to 11 times higher than the density reported by Deng and co-workers when immobilizing thrombin aptamers on monolithic columns [34]. Indeed, these authors reported an aptamer density of 0.568 nmol μL^{-1}. This high difference probably results from the percolation of a similar amount of aptamers (5.2 and 5.0 nmol against 5.7 nmol) for a much lower capillary volume in our case. It is indeed visible in Table 2 that the maximal coverage density (i.e., the ratio between the amount of percolated aptamers and the volume of the capillary, $Qty_{apt.\ perc.}/V_{cap}$) that could be reached is, respectively, equal to 6.6 and 6.3 nmol μL^{-1} for OTA and cocaine aptamers. This is 5 to 6 times higher than the value that can be estimated by the data provided by Deng et al., i.e., 1.2 nmol μL^{-1}. A grafting yield of about 48.9 % for thrombin aptamer was calculated with this value [34]. This yield is 1.7 and 2 times lower than the yields determined for cocaine and OTA aptamers. Grafting yields were indeed 96.4±1.6 and 83.3±9.1 % for both corresponding mOSs. This difference can be partly explained by the effect of the spacer length, that is longer in our study (Table 2), on the accessibility of the reactive amino group as previously reported by our group [6]. Moreover, no indication was given by Deng et al. on the duration of the activation step with glutaraldehyde. In previous studies of the same group [51], the capillary columns were activated for 6 h against 16 h in our case. A longer activation may increase the number of activated sites accessible for the immobilization, thus increasing the grafting yield of aptamers and the total amount of grafted aptamers. Other parameters, such as the temperature or the concentration of aptamers in the solution, may also have an impact.

To conclude, the aptamer density has been confirmed to be very high, thanks to the high specific surface area of the hybrid inorganic-organic monolith and seemed to be consistent with the grafting of thrombin aptamers previously reported. However, this experiment only allows estimating the amount of immobilized aptamers without any information about the ratio of active aptamers, i.e., aptamers that are able to selectively trap OTA. Indeed, some aptamers can be immobilized with a wrong orientation or fixed to the monolith at several points, i.e., through amino groups of nucleobases, preventing them to adopt the adequate conformation for the binding of OTA. Capacity measurements were thus carried out to evaluate the amount of active immobilized aptamers. The capacity corresponds to the maximal amount of OTA that can be retained by the mOS without loss of recovery. It is directly linked to the number of active and accessible aptamers grafted on the surface of the pores of the monolith. BB solutions (inj= 250 nL) spiked with increasing amounts of OTA, from 12.5 to 5.0 ng, were preconcentrated on-line on mOS_1 with a washing volume of 5.0 μL. This upper limit of 5 ng corresponded to the amount of OTA, above which, saturation of the detector was reached. No decrease of recoveries was observed for this concentration range. The capacity was therefore higher than 5.0 ng, i.e., superior to 22.5 pmol μL^{-1} active aptamers. This value is higher than for the grafting of antibodies. Indeed, a value of 0.543 pmol μL^{-1} of active

antibodies was previously reported by our group [36], i.e., at least 40 times lower than for aptamers. Aptamers are thus powerful tools to reach high capacities in comparison with antibodies because of their low size. Otherwise, Deng et al. reported a capacity of 1.95×10^{-24} mol nm^{-2}, i.e., 31.2 pmol μL^{-1} with a hybrid silica-based monolithic column (250 μm i.d.) [34], higher than the maximal value that could be measured with our LIF detector. This value is equal to 5.4 % of the density of grafted aptamers reported in the same work. For such a ratio, the capacity of a mOS would be equal to 338 pmol μL^{-1}, i.e., 56 ng OTA. This value is much higher than values reported for packed columns (33.8± 3.2 pmol μL^{-1} [18], 204±23 pmol μL^{-1} [21]) or open tubular capillaries (5.6 pmol μL^{-1} [23]) grafted with aptamers. This again highlights the high potential of the silica-based monolithic approach to reach a high binding capacity.

Selective oligoextraction from beer samples

The potential of the mOS was clearly demonstrated for the selective extraction of the model analyte from aqueous pure media. Extraction from a complex medium was then considered. OTA is generally determined in foodstuff such as cereal by-products [13], wine [14], or beer [52, 53]. To illustrate the selectivity in complex matrices, a beer sample, whose ethanol content (4.2 %) is known to potentially affect the retention mechanism, was chosen. Otherwise, the DNA aptamer takes its conformation in the presence of a divalent cation (i.e., Ca^{2+}). This implied to dilute the samples in BB. Cruz and co-workers [5] reported that the dissociation constant aptamer-OTA (K_D) is equal to 49±3 and 54±8 nM for Ca^{2+} concentrations, respectively, of 20 and 10 mM in solution. These two values are very similar; beer samples were thus diluted only once with BB (containing 20 mM Ca^{2+}) to obtain a final concentration of 10 mM Ca^{2+} and 2.1 % of ethanol in a mixture Beer/BB (50:50).

Beer/BB (50:50) and BB solutions spiked with increasing amounts of OTA (from 25 to 375 pg with an injection loop of 250 nL) were injected directly not only on the analytical column but also on mOS_4 coupled to nanoLC-LIF using the optimal washing volume of 6.0 μL that previously allowed obtaining the best selectivity and specificity. The chromatograms corresponding to injections of beer/BB samples spiked with 75 pg OTA are compared in Fig. 5 with chromatograms corresponding to the injection of spiked BB. The chromatogram corresponding to the direct injection of beer/BB sample (Fig. 5a) highlights the presence of many interfering compounds when comparing it with the chromatogram of spiked BB. A very intense peak around 6.5 min is observed corresponding to the numerous compounds contained in the beer. Furthermore, the retention time was delayed in comparison with BB spiked with OTA and its standard deviation increased. It was equal to 7.38±0.09 min in BB (n=7, RSD= 1.2 %) against 9.91±0.88 min in a mixture beer/BB (n=7, RSD=8.9 %). For comparison, OTA in spiked pure water (not shown in this figure, see Electronic Supplementary Material (ESM)) presented a retention time of 6.77±0.07 min (n=7, RSD=1.1 %). The shift may be thus attributed to a modification of the interactions with the analytical column due to the modification of the buffer composition and particularly of the pH of the injected solution. Indeed, the pH of the mixture beer/BB is about 4.5 against a pH of 5.4 for BB. The pKa of the carboxylic moiety of OTA is about 4.4; the protonated form of OTA is thus more present in beer/BB than in BB, thus favoring its retention in reversed phase mode. On the contrary, the comparison between injection of spiked BB and injection of the beer/BB sample preconcentrated on the mOS (Fig. 5b) confirms that interfering compounds were mostly eliminated during the percolation and washing steps on the mOS while

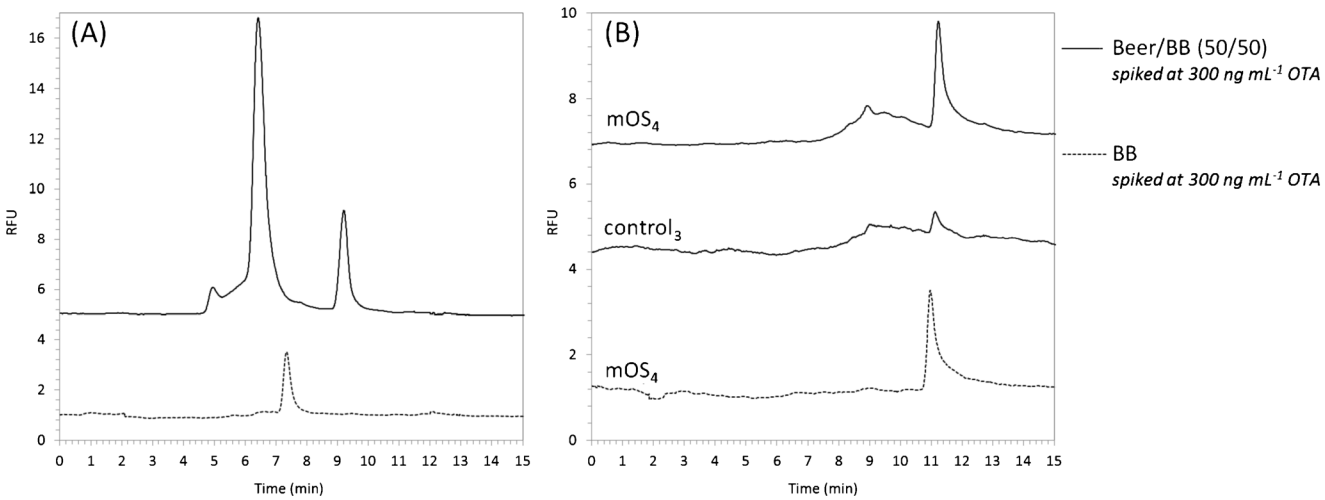

Fig. 5 NanoLC chromatograms corresponding to the analysis of 250 nL of beer/BB (50:50) and BB spiked with 75 pg OTA. **A** Direct injection of each sample on the analytical column. **B** Extraction of each sample on mOS_4 and $control_3$ coupled on-line with nanoLC-LIF

OTA was on the contrary selectively retained on the device. No shift of the retention time was observed in comparison with injections of BB spiked with OTA. Indeed, when the second nano-valve is switched to elute OTA retained in the mOS, OTA is contained in BB, i.e., the washing solvent, whatever the initial sample composition (beer/BB or BB). Furthermore, OTA is not retained on the control device even in complex samples.

Otherwise, by comparing the chromatograms corresponding to the BB and beer/BB samples in Fig. 5a, it can be noticed that the matrix affects also the peak area when injecting the samples directly on the analytical column. To illustrate this point, the curves corresponding to the obtained peak area as a function of the amount of OTA are gathered in Fig. 6. It is visible that a direct injection of beer/BB spiked with OTA on the column caused a strong increase of the peak area compared with injections of OTA in BB. A slope of 0.0164 was obtained in the first case against 0.0097 in the second, i.e., 1.7 times lower. Injections of pure water spiked with OTA were also carried out (not shown here, see ESM) and led to a slope 1.5 times lower than in BB. As for the retention time, the composition of the buffer may have a strong influence on the fluorescence properties of OTA as reported previously [54, 55]. This can interfere with the quantification of OTA. On the contrary, when purifying the sample by injecting those same samples on the device mOS/nanoLC-LIF, the peak area obtained with Beer/BB was similar to the peak areas obtained with OTA in BB. The slopes of the two curves are not significantly different (t test, $p=0.12>0.05$) which is highlighted by the superposition of the 95 % confidence bands of the two sets of data in Fig. 6b. The extraction recovery can be thus estimated to be comprised between 90 and 99 % in those two kinds of matrices. This is consistent with the recovery yields obtained previously (Fig. 4b) with a washing of 6.0 μL for a pure BB spiked with OTA, thus highlighting the fact that the matrix has no effect on the aptamer binding. Therefore, a high level of purification can be achieved by the on-line coupling of a mOS specific for a target molecule with nanoLC by using very low amounts of samples.

Finally, more than 50 injections were achieved on the mOSs without observing loss of retention after percolation of both pure and complex samples, thus showing the stability of this sorbent. The chosen monolithic approach followed by covalent grafting of aptamers allowed obtaining a stable device for on-line selective preconcentration of small molecules. In the case of OTA, our model analyte, the extraction of the molecule from red wine or wheat extracts, could be now considered.

Conclusions and perspectives

An innovative approach to miniaturize a selective DNA-aptamer-based extraction sorbent was described. We have demonstrated that a sol-gel approach can be used to immobilize a DNA aptamer and develop a miniaturized oligosorbent coupled on-line to nanoLC. The reproducibility of the monolith synthesis and further grafting of aptamer were more particularly highlighted. The selective extraction of a model analyte for which an aptamer was available was successfully carried out. The extraction procedure developed in pure aqueous solutions led to high and reproducible extraction recovery. Furthermore, the measured aptamer coverage density and binding capacity were high in comparison with aptamer-immobilized open tubular capillaries or packed columns. This miniaturized device was then successfully applied to the extraction of the model analyte, OTA, from few hundred

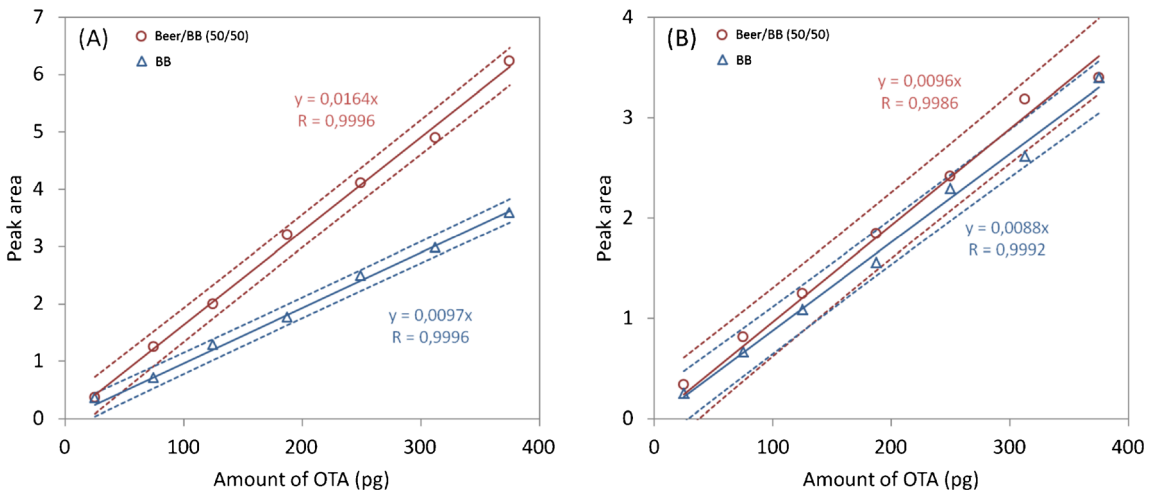

Fig. 6 Peak area of OTA obtained by LIF detection as a function of the amount of injected OTA in two kinds of samples: beer/BB 50:50 (*circle*) and BB (*triangle*). **A** Direct injection on the analytical column. **B** Oligoextraction on mOS_4 coupled on-line with nanoLC. *Dashed line*: 95 % confidence bands

nanoliters of beer samples. This paper constitutes a proof of concept of an approach that could be now easily adapted for the development of other mOSs by just changing the nature of the grafted aptamers and the type of detection.

Acknowledgments This work was supported by the French National Research Agency (ANR Program CESA 2010, Mycodiag Project).

References

1. Hennion M-C, Pichon V (2003) Immuno-based sample preparation for trace analysis. J Chromatogr A 1000(1–2):29–52
2. Delaunay N, Pichon V, Hennion M-C (2000) Immunoaffinity solid-phase extraction for the trace-analysis of low-molecular-mass analytes in complex sample matrices. J Chromatogr B Biomed Appl 745(1):15–37
3. Delaunay-Bertoncini N, Pichon V, Hennion MC (2001) Immunoextraction: a highly selective method for sample preparation. LC-GC 14(3):162–172
4. Pichon V, Chapuis-Hugon F, Hennion MC (2012) 2.19—bioaffinity sorbents. In: Pawliszyn J (ed) Comprehensive sampling and sample preparation, volume 2: theory of extraction techniques, vol 2. Academic, Oxford, pp 359–388
5. Cruz-Aguado JA, Penner G (2008) Determination of ochratoxin A with a DNA aptamer. J Agric Food Chem 56(22):10456–10461
6. Madru B, Chapuis-Hugon F, Pichon V (2011) Novel extraction supports based on immobilised aptamers: evaluation for the selective extraction of cocaine. Talanta 85(1):616–624
7. Madru B, Chapuis-Hugon F, Peyrin E, Vr P (2009) Determination of cocaine in human plasma by selective solid-phase extraction using an aptamer-based sorbent. Anal Chem 81(16):7081–7086
8. Stoltenburg R, Reinemann C, Strehlitz B (2007) SELEX—a (r)evolutionary method to generate high-affinity nucleic acid ligands. Biomol Eng 24(4):381–403
9. Luzi E, Minunni M, Tombelli S, Mascini M (2003) New trends in affinity sensing: aptamers for ligand binding. TrAC Trends Anal Chem 22(11):810–818
10. Brumbt A, Ravelet C, Grosset C, Ravel A, Villet A, Peyrin E (2005) Chiral stationary phase based on a biostable l-RNA aptamer. Anal Chem 77(7):1993–1998
11. Deng Q, Watson CJ, Kennedy RT (2003) Aptamer affinity chromatography for rapid assay of adenosine in microdialysis samples collected in vivo. J Chromatogr A 1005(1–2):123–130
12. Romig TS, Bell C, Drolet DW (1999) Aptamer affinity chromatography: combinatorial chemistry applied to protein purification. J Chromatogr B Biomed Appl 731(2):275–284
13. Hadj Ali W, Pichon V (2014) Characterization of oligosorbents and application to the purification of ochratoxin A from wheat extracts. Anal Bioanal Chem 406(4):1233–1240
14. Chapuis-Hugon F, Boisbaudry A, Madru B, Pichon V (2011) New extraction sorbent based on aptamers for the determination of ochratoxin A in red wine. Anal Bioanal Chem 400(5):1199–1207
15. Michaud M, Jourdan E, Villet A, Ravel A, Grosset C, Peyrin E (2003) A DNA aptamer as a new target-specific chiral selector for HPLC. J Am Chem Soc 125(28):8672–8679
16. Michaud M, Jourdan E, Ravelet C, Villet A, Ravel A, Grosset C, Peyrin E (2004) Immobilized DNA aptamers as target-specific chiral stationary phases for resolution of nucleoside and amino acid derivative enantiomers. Anal Chem 76(4):1015–1020
17. Ravelet C, Boulkedid R, Ravel A, Grosset C, Villet A, Fize J, Peyrin E (2005) A l-RNA aptamer chiral stationary phase for the resolution of target and related compounds. J Chromatogr A 1076(1–2):62–70
18. Ruta J, Ravelet C, Désiré J, Décout J-L, Peyrin E (2008) Covalently bonded DNA aptamer chiral stationary phase for the chromatographic resolution of adenosine. Anal Bioanal Chem 390(4):1051–1057
19. Cho S, Lee S-H, Chung W-J, Kim Y-K, Lee Y-S, Kim B-G (2004) Microbead-based affinity chromatography chip using RNA aptamer modified with photocleavable linker. Electrophoresis 25(21–22): 3730–3739
20. Chung W-J, Kim M-S, Cho S, Park S-S, Kim J-H, Kim Y-K, Kim B-G, Lee Y-S (2005) Microaffinity purification of proteins based on photolytic elution: toward an efficient microbead affinity chromatography on a chip. Electrophoresis 26(3):694–702
21. Deng Q, German I, Buchanan D, Kennedy RT (2001) Retention and separation of adenosine and analogues by affinity chromatography with an aptamer stationary phase. Anal Chem 73(22):5415–5421
22. Zhang YP, Zhang YJ, Gong WJ, Chen N, Gopalan A-I, Lee KP (2010) Novel fabrication of on-column capillary inlet frits through flame induced sintering of stainless steel particles. Microchem J 95(1):67–73
23. Connor AC, McGown LB (2006) Aptamer stationary phase for protein capture in affinity capillary chromatography. J Chromatogr A 1111(2):115–119
24. Rehder MA, McGown LB (2001) Open-tubular capillary electrochromatography of bovine β-lactoglobulin variants A and B using an aptamer stationary phase. Electrophoresis 22(17):3759–3764
25. Rehder-Silinski MA, McGown LB (2003) Capillary electrochromatographic separation of bovine milk proteins using a G-quartet DNA stationary phase. J Chromatogr A 1008(2):233–245
26. Clark SL, Remcho VT (2003) Open tubular liquid chromatographic separations using an aptamer stationary phase. J Sep Sci 26(15–16): 1451–1454
27. Kotia RB, Li L, McGown LB (2000) Separation of nontarget compounds by DNA aptamers. Anal Chem 72(4):827–831
28. Charles JAM, McGown LB (2002) Separation of Trp-Arg and Arg-Trp using G-quartet-forming DNA oligonucleotides in open-tubular capillary electrochromatography. Electrophoresis 23(11):1599–1604
29. Clark SL, Remcho VT (2003) Electrochromatographic retention studies on a flavin-binding RNA aptamer sorbent. Anal Chem 75(21):5692–5696
30. Dick LW Jr, Swinteck BJ, McGown LB (2004) Albumins as a model system for investigating separations of closely related proteins on DNA stationary phases in capillary electrochromatography. Anal Chim Acta 519(2):197–205
31. Gao C, Sun X, Woolley AT (2013) Fluorescent measurement of affinity binding between thrombin and its aptamers using on-chip affinity monoliths. J Chromatogr A 1291:92–96
32. Zhao Q, Li X-F, Le XC (2008) Aptamer-modified monolithic capillary chromatography for protein separation and detection. Anal Chem 80(10):3915–3920
33. Zhao Q, Li X-F, Shao Y, Le XC (2008) Aptamer-based affinity chromatographic assays for thrombin. Anal Chem 80(19):7586–7593
34. Deng N, Liang Z, Liang Y, Sui Z, Zhang L, Wu Q, Yang K, Zhang L, Zhang Y (2012) Aptamer modified organic–inorganic hybrid silica monolithic capillary columns for highly selective recognition of thrombin. Anal Chem 84(23):10186–10190
35. Xu L, Shi Z-G, Feng Y-Q (2011) Porous monoliths: sorbents for miniaturized extraction in biological analysis. Anal Bioanal Chem 399(10):3345–3357
36. Brothier F, Pichon V (2013) Immobilized antibody on a hybrid organic–inorganic monolith: capillary immunoextraction coupled on-line to nanoLC-UV for the analysis of microcystin-LR. Anal Chim Acta 792:52–58
37. Mosesso P, Cinelli S, Piñero J, Bellacima R, Pepe G (2008) In vitro cytogenetic results supporting a DNA nonreactive mechanism for ochratoxin A, potentially relevant for its carcinogenicity. Chem Res Toxicol 21(6):1235–1243

38. Muñoz K, Vega M, Rios G, Muñoz S, Madariaga R (2006) Preliminary study of ochratoxin A in human plasma in agricultural zones of Chile and its relation to food consumption. Food Chem Toxicol 44(11):1884–1889
39. Turner NW, Subrahmanyam S, Piletsky SA (2009) Analytical methods for determination of mycotoxins: a review. Anal Chim Acta 632(2):168–180
40. Kabak B (2009) Ochratoxin A in cereal-derived products in Turkey: occurrence and exposure assessment. Food Chem Toxicol 47(2): 348–352
41. Pfohl-Leszkowicz A, Manderville RA (2007) Ochratoxin A: an overview on toxicity and carcinogenicity in animals and humans. Mol Nutr Food Res 51(1):61–99
42. Barthelmebs L, Hayat A, Limiadi AW, Marty J-L, Noguer T (2011) Electrochemical DNA aptamer-based biosensor for OTA detection, using superparamagnetic nanoparticles. Sensors Actuators B 156(2): 932–937
43. Chen J, Fang Z, Liu J, Zeng L (2012) A simple and rapid biosensor for ochratoxin A based on a structure-switching signaling aptamer. Food Control 25(2):555–560
44. De Girolamo A, McKeague M, Miller JD, DeRosa MC, Visconti A (2011) Determination of ochratoxin A in wheat after clean-up through a DNA aptamer-based solid phase extraction column. Food Chem 127(3):1378–1384
45. Soler-Illia GJAA, Sanchez C, Lebeau B, Patarin J (2002) Chemical strategies to design textured materials: from microporous and mesoporous oxides to nanonetworks and hierarchical structures. Chem Rev 102(11):4093–4138
46. Wight AP, Davis ME (2002) Design and preparation of organic–inorganic hybrid catalysts. Chem Rev 102(10):3589–3614
47. Hoffmann F, Cornelius M, Morell J, Fröba M (2006) Silica-based mesoporous organic–inorganic hybrid materials. Angew Chem Int Ed 45(20):3216–3251
48. Hoffmann F, Froba M (2011) Vitalising porous inorganic silica networks with organic functions-PMOs and related hybrid materials. Chem Soc Rev 40(2):608–620
49. Mehdi A, Reye C, Corriu R (2011) From molecular chemistry to hybrid nanomaterials. Design and functionalization. Chem Soc Rev 40(2):563–574
50. Zhu T, Row KH (2012) Preparation and applications of hybrid organic–inorganic monoliths: a review. J Sep Sci 35(10–11):1294–1302
51. Ma J, Liang Z, Qiao X, Deng Q, Tao D, Zhang L, Zhang Y (2008) Organic–inorganic hybrid silica monolith based immobilized trypsin reactor with high enzymatic activity. Anal Chem 80(8):2949–2956
52. Rhouati A, Hayat A, Hernandez DB, Meraihi Z, Munoz R, Marty J-L (2013) Development of an automated flow-based electrochemical aptasensor for on-line detection of ochratoxin A. Sensors Actuators B 176:1160–1166
53. Rhouati A, Paniel N, Meraihi Z, Marty J-L (2011) Development of an oligosorbent for detection of ochratoxin A. Food Control 22(11): 1790–1796
54. Bazin I, Faucet-Marquis V, Monje M-C, El Khoury M, Marty J-L, Pfohl-Leszkowicz A (2013) Impact of pH on the stability and the cross-reactivity of ochratoxin A and citrinin. Toxins 5(12):2324–2340
55. Dohnal V, Pavlíková L, Kuca K (2010) The pH and mobile phase composition effects ochratoxin A fluorescence at liquid chromatography. J Chromatogr Sci 48(9):766–770